DOE/PC/88867--T5

DE90 006171

DOE/PC/88867-T5
(SRI-ENV-89-1054-6657-16)
(DE90006171)
Distribution Category UC-105

ELECTROSTATIC PRECIPITATION OF CONDENSED ACID MIST

Phase I Final Report
(September 1988 to September 1989)

Robert S. Dahlin
Southern Research Institute
2000 Ninth Avenue South
P. O. Box 55305
Birmingham, Alabama 35255-5305

Thomas D. Brown, Technical Project Officer
Pittsburgh Energy Technology Center
P. O. Box 10940
Pittsburgh, Pennsylvania 15236-0940

Prepared for the

U.S. Department of Energy
Under Contract No. DE-AC22-88PC88867

SRI-ENV-89-1054-6657-XVI
November 1989

ABSTRACT

Under contract to the Department of Energy, Southern Research Institute is developing a compact, wet electrostatic precipitator (WESP) to control acid mist emissions from high-sulfur coal combustion. The WESP is being developed as a retrofit technology for existing coal-fired power plants, particularly those equipped with wet flue gas desulfurization (FGD) scrubbers. Acid mist emissions can be a significant problem at these facilities because the sulfuric acid vapor in the flue gas is converted to a very fine mist that is not collected in the scrubber system. Conventional mist eliminators are not adequate in this application due to the very fine size of the mist droplets. The potential for corrosion also makes it difficult to use a fabric filter or a conventional, dry ESP in this application. Therefore, this research project has been structured around the development of a compact WESP that could be retrofit on top of an existing scrubber or within an existing flue gas duct.

This paper describes the development and testing of a prototype WESP for the utility acid mist application. The fractional collection efficiency of the WESP was first evaluated in the laboratory using a simulant aerosol produced by atomizing a non-volatile oil. After successful completion of these tests, the performance of the WESP was evaluated using an actual acid mist produced in a pilot combustion facility equipped with a spray humidification chamber. Testing was conducted with combustion of sulfur-doped gas to simulate the acid mist alone, and with a combination of coal and sulfur-doped gas to simulate the mixture of acid mist and fly ash downstream from a scrubber. Without the resistivity limitations of a dry ESP, the WESP could be operated reliably at current densities that were 2 to 7 times higher than those of a typical dry ESP. This enabled the WESP to achieve reasonably good control efficiency (82.5 to 84.5% for mist alone and 77.6% for the mist/fly ash combination) with a specific collection area that was 4 to 8 times smaller than that of a typical dry ESP.

The performance of the WESP test unit was modeled using two different cylindrical-geometry computer models: a "current-seeking" model and a "current-specific" model. The current-seeking model was found to be unsuitable because the equation used to predict the current applies only in the region near corona start. The current-specific model yielded predicted overall collection efficiencies that were in substantial agreement with the measured efficiencies for the mist-only case. For the mist plus ash case, agreement was good after correction of the data for collection of larger ash particles in the mist eliminator. Use of the current-specific model to simulate a commercial WESP installation suggests that an overall efficiency of 86.7% may be possible with a SCA of 50 ft^2/kacfm and a gas velocity of 20 ft/sec. A unit of this size could be retrofitted on top of an existing scrubber.

FIGURES

TABLES

ACKNOWLEDGMENTS

The following individuals contributed to the successful completion of this project through their roles in the WESP development and testing program.

John D. Carlton	-	Assembly and lab testing, impactor sampling
Sherry S. Dawes	-	Data reduction
M. Greg Faulkner	-	Computer modeling
John P. Gooch	-	Data review and analysis
J. Sam O'Neal	-	Lab testing, impactor sampling
Kenneth D. O'Neal	-	Assembly and combustor testing, impactor sampling
Grady B. Nichols	-	Technical review and consultation
William J. Page	-	Assembly and combustor testing, impactor sampling
Jill V. Pate	-	Report preparation
Michael S. Robinson	-	Combustor testing, impactor sampling
Todd R. Snyder	-	Combustor testing, impactor sampling
Lee Ann Wallace	-	Impactor substrate weighing

CONTENTS

ELECTROSTATIC PRECIPITATION OF CONDENSED ACID MIST

1. INTRODUCTION

This project addresses the acid mist that is formed by condensation of sulfuric acid vapor in flue gas from coal-fired utility boilers. An acid mist can be formed whenever the flue gas temperature approaches the prevailing acid dew point. This commonly occurs when the gas is subjected to rapid adiabatic cooling in a wet scrubber system for flue gas desulfurization. Acid mists can also sometimes result from unexpected temperature excursions caused by air inleakage, load cycling, and start-up operations.

Most of the acid mist that is formed in a wet scrubber system escapes collection in the scrubber (1). This is a result of the extremely fine droplet size in the acid mist, which allows the mist droplets to follow the gas streamlines around the droplets of scrubber slurry, thereby avoiding collection by inertial impaction or interception.

Acid mists can sometimes constitute a significant portion of the total particulate emissions from power plants burning high-sulfur coals. Complete condensation of 10 ppm of acid vapor produces a condensed acid mass loading of about 0.02 gr/dscf or 0.03 lb/MMBtu, equivalent to the total allowable mass emissions under the revised (1979) New Source Performance Standards (2).

In some states, the mass emission sampling protocols allow exclusion of the acid mass from the total particulate sample (cf 3). Even in these cases, the acid mist can be a limiting factor due to its effect on opacity. The acid mist droplets are predominantly in the size range of 0.1 to 1 μm (4), where light scattering is very efficient. In some cases, the droplet size distribution seems to be concentrated in the 0.4 to 0.5 μm range, near the wavelength of blue light, giving the plume a bluish tint (5). Due to these considerations, it may be necessary to reduce acid mist emissions even when their contribution to the total particulate mass is relatively small.

A wet electrostatic precipitator (WESP) is the best control option for acid mist. The mist would blind a fabric filter and attack glass fiber fabrics. A wet ESP is required because the acid would quickly corrode the plates in a conventional dry ESP. The wet ESP also offers the advantages of no rapping reentrainment and no sensitivity to fly ash resistivity. Therefore, this program has been structured around the use of a compact, wet ESP to control acid mist emissions.

2. OBJECTIVES AND SCOPE OF WORK

The purpose of this project is to develop and demonstrate a compact, wet electrostatic collector for condensed acid mist in power plant flue gas. In order to accomplish this goal, several objectives must be met.

1. A laboratory-version of the WESP must be fabricated.

2. The WESP performance must be optimized through laboratory tests with a non-volatile simulant aerosol having a size distribution similar to the acid mist.

3. The WESP concept must be proven by demonstrating adequate collection of actual acid mist in a pilot coal combustion facility under conditions simulating a full-scale power plant burning high-sulfur coal.

4. A computer model of the WESP process must be developed to assist in the process optimization, interpretation of test results, and extrapolation to full scale.

5. Utility participation must be solicited in a follow-on demonstration of the WESP concept at a full-scale power plant.

The project is organized in two phases. Phase I, which was conducted from September 1988 to September 1989, involved the WESP fabrication, laboratory and pilot combustor testing, and computer modeling. Phase II, which is scheduled for September 1989 to September 1990, involves the solicitation of a utility demonstration site, preliminary site measurements, and planning for the demonstration test program. The execution of Phase II is contingent upon successful completion of Phase I. Only Phase I has been funded at this time. Therefore, only the Phase I work will be addressed in this discussion.

Phase I is organized in five tasks, with two of the tasks having subtasks as follows:

Task 1. Work Plan Preparation

Task 2. Hardware and Software Development

Subtask 2.1. Prototype ESP fabrication
Subtask 2.2. ESP model development

Task 3. Laboratory Testing

Subtask 3.1. Preparation of auxiliary systems
Subtask 3.2. Tests of collection efficiency

Task 4. Pilot Combustor Testing

Task 5. Phase I Reporting

3. LABORATORY TESTS OF WESP WITH SIMULANT AEROSOL

The prototype WESP system used in the laboratory tests was basically a modification of a cylindrical ESP used previously in studying the collection of acid mists from chrome plating baths. Figures 1 and 2 show a sketch and a photograph of the system.

A simulated acid mist was produced by atomizing a non-volatile, non-toxic simulant liquid, di (2-ethylhexyl) sebacate (DES). This liquid was atomized using a Sonic Development ST-47 nozzle. When operated at the upper limit of atomizing air pressure, the nozzle produced droplets in the desired size range to simulate an acid mist. Even though the size distribution of the mist was slightly coarse compared to an actual acid mist, the necessary data on fine particle collection could still be obtained by size-resolved impactor measurements at the ESP inlet and outlet.

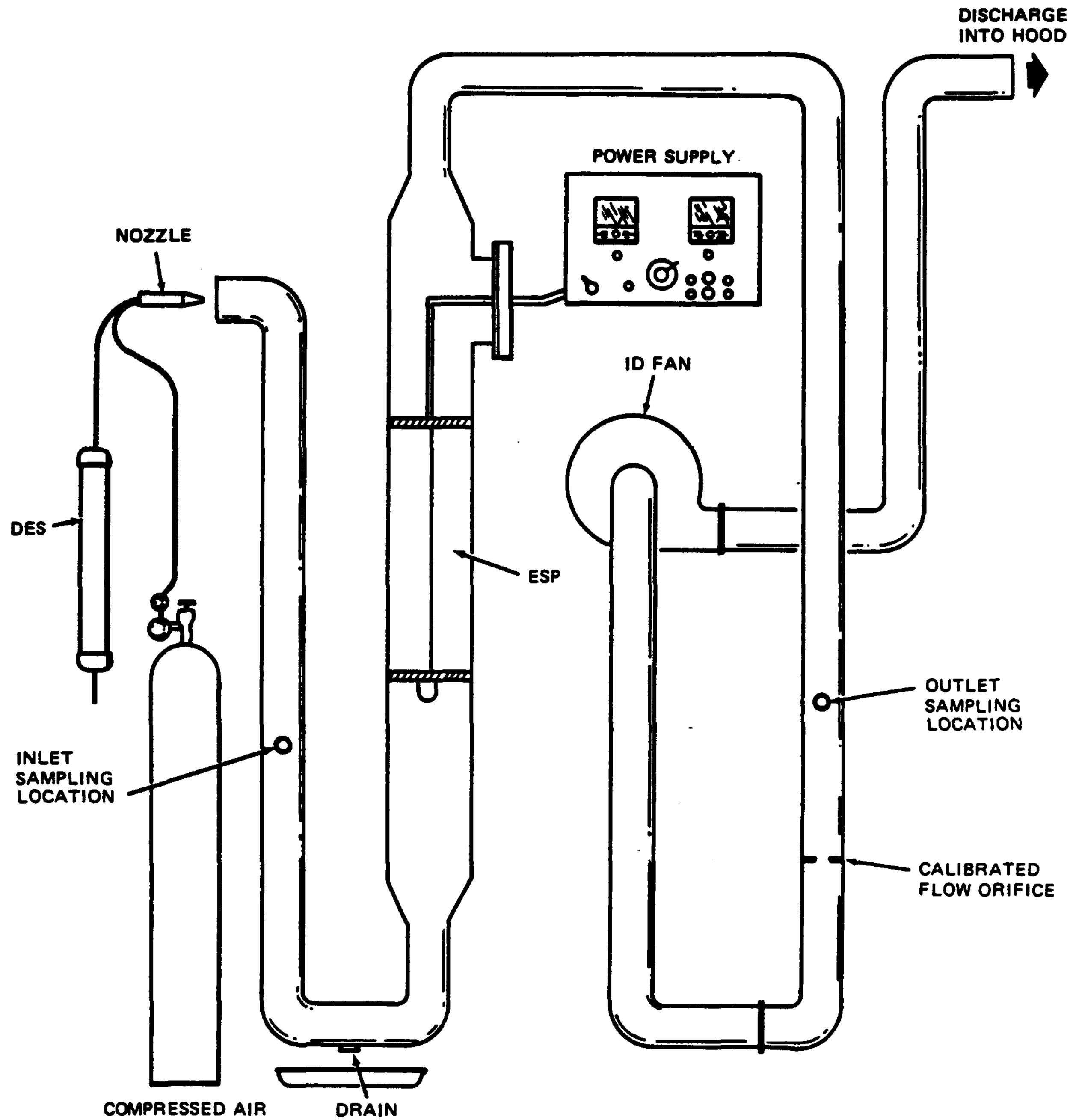

Figure 1. Sketch of Prototype ESP System.

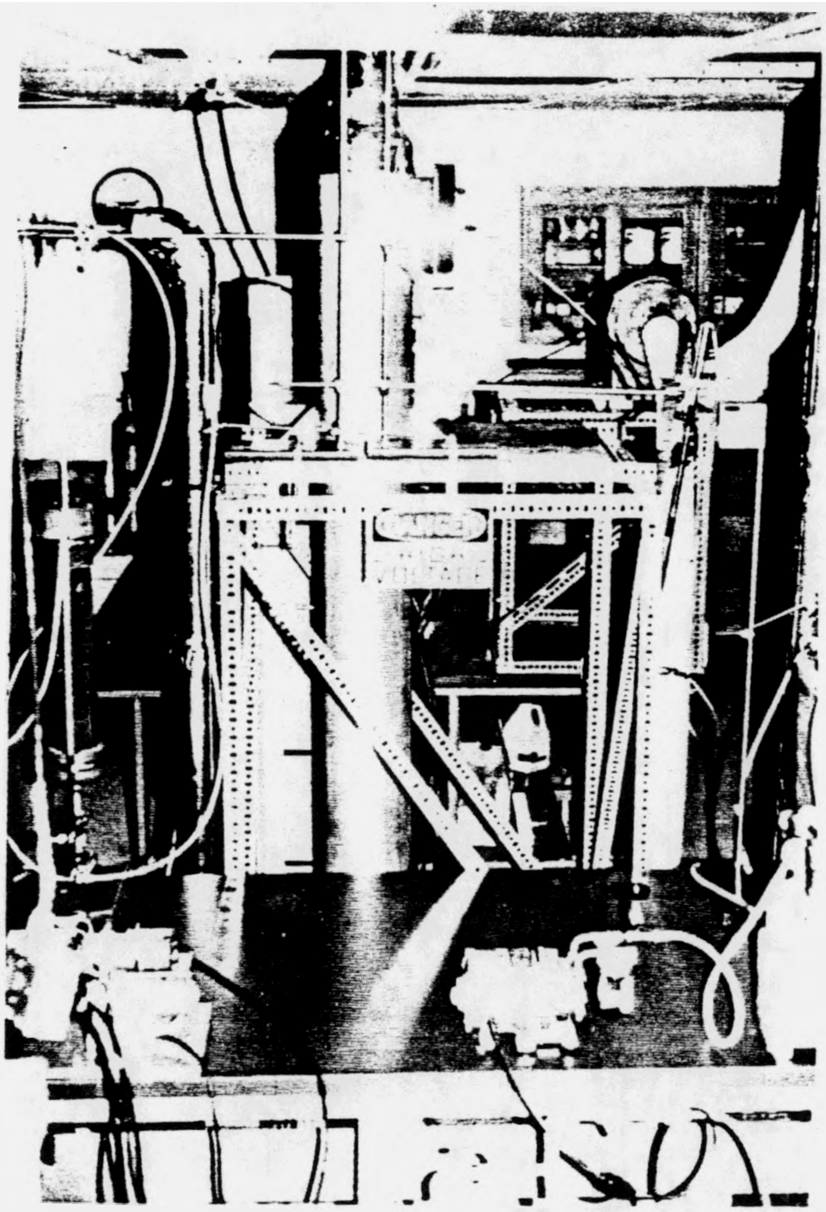

Figure 2. Photograph of the Prototype ESP System.

The DES aerosol was drawn into a flow of ambient air that was pulled through the system using a Dayton Model 2C940 1/3 HP blower as an ID fan. The maximum air flow through the system with this blower was about 97 acfm at ambient conditions. This produced a nominal gas velocity of 4.5 ft/sec through the ESP, which had a diameter of 8 in. This velocity is typical for modern dry ESP designs, but is somewhat low for a WESP. However, since an actual utility installation would be much taller, the residence time in the ESP is more representative of actual practice.

The ducts channeling the air to and from the ESP were fabricated from standard 4-in. galvanized ducting, commonly used to vent home water heaters. The velocity in these ducts was about 18 ft/sec, which was sufficient to prevent dropout in the ductwork. The velocity could have been increased by using smaller ductwork, but this would have made impactor sampling difficult.

The ESP itself consisted of a single 1/8-in. smooth wire suspended along the centerline of an 8-in. diameter thin-wall pipe. The wire was rigidly mounted using an insulating standoff assembly at each end. The total length of energized wire was 42 in., yielding an effective specific collection area (SCA) of about 75 ft^2 per 1000 acfm of air flow. This SCA would be quite low for a conventional dry ESP, but is a reasonable design point for a WESP.

The ESP was energized by a single Hipotronics Model 860A 60-kV dc power supply. In previous operation of the ESP with a 50-kV power supply, an operating current of 1.2 mA was achieved at maximum output with air flow only. With DES atomized into the air to produce a loading of about 0.8 gr/acf, the operating current was reduced to 0.8 mA. No sparking was observed in either operating mode. These operating conditions correspond to current densities of 164 and 109 $\mu A/ft^2$, which are quite high for conventional ESP applications, and illustrate the potentially favorable conditions for acid mist collection.

The laboratory WESP system included all necessary auxiliary systems for impactor sampling at the ESP inlet and outlet. The inlet sampling port was located approximately 7 ft downstream from the atomizing nozzle and 5 ft upstream from the ESP. The outlet sampling port was originally located approximately 9 ft downstream from the ESP and 12 ft upstream from the ID fan. A flow measurement orifice was located about 1 ft downstream from the outlet sampling port. After initial startup of the laboratory ESP system, the outlet ductwork was modified to change from a flexible hose to a rigid design. With the modified outlet ductwork, the outlet sampling port was relocated to a point 13 ft downstream from the ESP. The flow measurement orifice was relocated to a point about 2 ft downstream from the outlet sampling port.

Manometer boards, calibrated orifices, gas meters, and pumps were set up to meter flow through the impactors. Originally, modified Brink impactors were used at both the inlet and outlet of the ESP. However, due to low outlet mass loadings, the type of impactor used at the outlet was switched from a low flowrate Brink impactor to a high-flowrate University of Washington impactor. This allowed both impactors to be run for the same time period without over-loading any of the impactor stages.

Collection efficiency as a function of particle size was determined by cascade impactor measurements using the Brink impactors at the inlet and the University of Washington impactors at the outlet. The inlet and outlet impactors were run simultaneously for a period of either 4 or 5 hours of steady-state ESP operation. Four sets of inlet and outlet runs were obtained. During all runs, the ESP was operated at maximum power input (60 kV and 2.3 mA). The air flow through the system was maintained constant at about 100 acfm. Atomizing air and DES pressures at the nozzle were maintained at 88 psig and 10 psig.

Excellent electrical operating conditions were achieved in the laboratory ESP, in that the 60 kV applied voltage resulted in a current density of over 300 microamps/ft^2. Although these conditions do not represent an optimum use of electrical power, the relatively high values of charging and collecting fields produced in the precipitator would be expected to result in high values of collection efficiency. An analysis of the initial impactor data confirmed this expectation in that overall collection efficiency ranged from a low of 99.14% to a high of 99.68%.

A second set of impactor data resolved some earlier operating difficulties and confirmed the initial data. Collection efficiency as a function of particle size was again determined by cascade impactor measurements using Brink impactors at the inlet and University of Washington impactors at the outlet. The inlet and outlet impactors were run simultaneously for a period of 4 hours of steady-state ESP operation. Four sets of inlet and outlet runs were obtained. During all runs, the ESP was operated at maximum power input (60 kV and 2 mA). The air flow through the system was again maintained constant at about 100 acfm. Atomizing air and DES pressures at the nozzle were again maintained at 88 psig and 10 psig.

Excellent electrical operating conditions were again achieved in the laboratory ESP, in that the 60 kV applied voltage resulted in a current density of 270 microamps/ft^2 (about 5 to 10 times higher than that of a typical dry ESP). Again, these conditions do not represent an optimum use of electrical power, but the relatively high values of charging and collecting fields produced in the precipitator resulted in high values of collection efficiency (from a low of 98.76% to a high of 98.92%). These values were slightly lower than the initial data, but still well above the desired performance.

Figure 3 shows the inlet and outlet cumulative mass loading curves. A comparison of the two curves over the particle size range resolved by the impactor reveals that 1) for the lower limit of particle size resolution, the cumulative loading at the outlet is lower than that at the inlet by a factor of about 16, and 2) for the upper limit of size resolution, the difference is a factor of about 60. For all particle sizes resolved by the impactors, the overall collection efficiency is 98.3%. The true overall collection efficiency is higher due to the large loading of droplets beyond the upper limit of impactor size resolution.

Figure 4 shows the fractional collection efficiency curve generated from the impactor data. As expected, the curve shows a strong dependence on particle size. Over the range of impactor size resolution, the efficiency varies from about 97.4% to 99.77%. This indicates excellent removal of the fine droplets expected to occur in an acid mist.

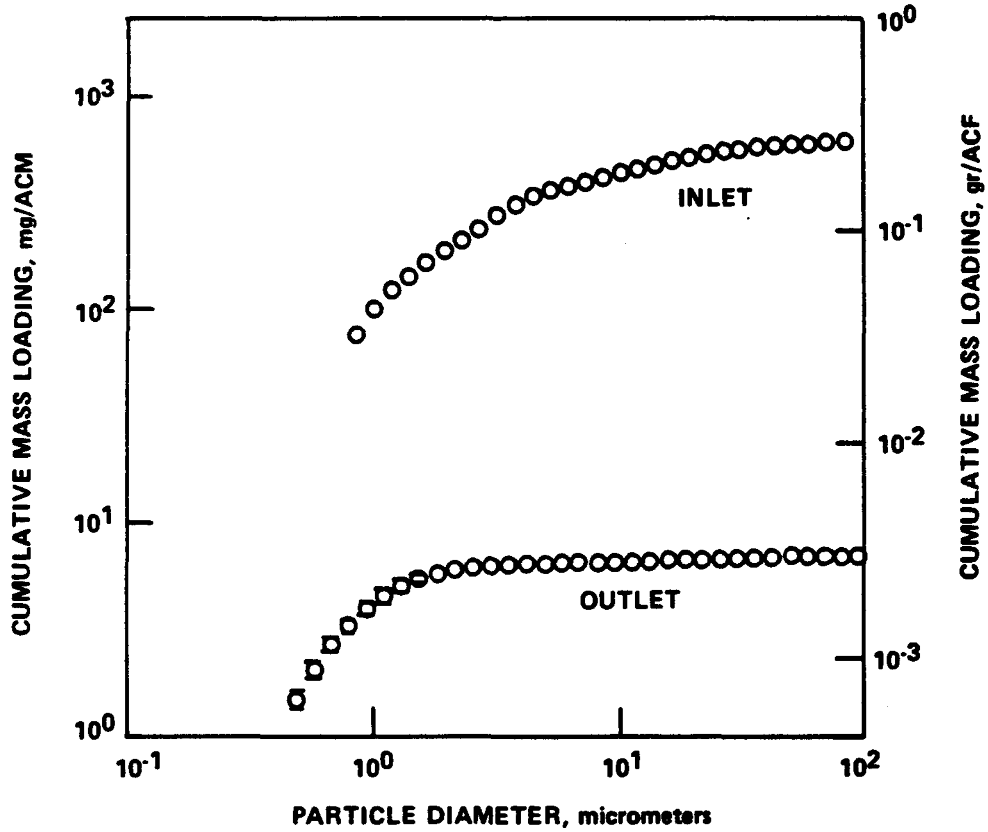

Figure 3. Comparison of Cumulative Mass Loading Curves Obtained at WESP Inlet and Outlet with Simulant Aerosol in Laboratory Tests.

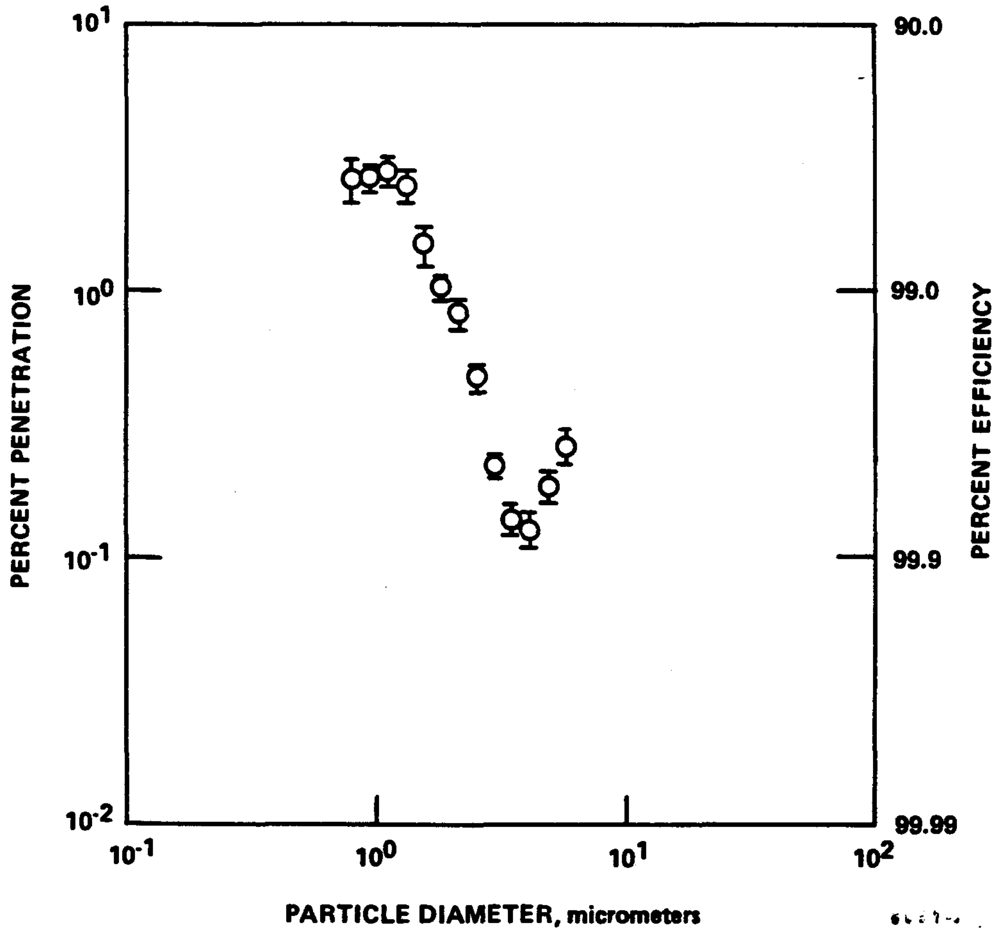

Figure 4. Fractional Collection Efficiency Curve Determined from Inlet and Outlet Impactor Runs with Simulant Aerosol in Laboratory Tests.

4. PILOT COMBUSTOR TESTS OF WESP WITH ACTUAL ACID MIST

The prototype WESP system was described in detail in Section 3. Substantial modifications were made to allow use of the prototype WESP system in the pilot combustion facility. As illustrated in Figure 5, the modified system incorporated a hot air purge and modified support system for the high-voltage insulator. A mesh-pad mist eliminator was also installed to eliminate any large water droplets that failed to evaporate. On a previous project, it was shown that this mist eliminator would not affect the concentration of droplets in the acid mist size range (below 1 μm). Also, the standoffs used in the laboratory WESP system were eliminated to avoid problems with tracking.

The sampling points used in the modified WESP system are shown in Figure 5. The new sampling system included three inlet impactor setups (two real and one blank) and two outlet impactors (both real). As in the lab tests, Brink impactors were used at the inlet, and University of Washington impactors were used at the outlet. The initial setup was later changed to use University of Washington impactors for the blanks, since they have a larger substrate surface area and, therefore, greater potential for vapor-phase interferences.

4.1 Tests with Acid Mist Only

For these tests, an acid mist was produced by combustion of SO_2-doped natural gas in the SRI one-million-Btu/hr pilot combustion system. The gas was doped with about 2200 ppm of SO_2, producing an SO_3 concentration of 24-26 ppm. This SO_3 was converted to a condensed acid mist by passing the flue gas through a spray humidification chamber. The gas was humidified to a 20-30°F approach to saturation so that all of the acid could be condensed without bulk condensation of water vapor in the WESP system. This resulted in a flue gas temperature of 135-145°F at the WESP inlet. There was a very slight temperature drop (typically < 5°F) across the WESP. The purge system was effective in preventing tracking along the high-voltage insulator, but the hot air produced an effective dilution of the flue gas entering the WESP. The inlet and outlet flue gas flowrates, based on pitot measurements, were 52-67 scfm (78-106 acfm) and 99-128 scfm (143-189 acfm). Thus, the hot-air purge accounted for about 50% of the system flow. This dilution factor has been taken into account in determining the WESP inlet mass loadings and collection efficiency.

Two sets of fractional efficiency tests were conducted with two different acid mist loadings, during the weeks of August 14 and August 28. During each day of testing, three Brink impactors (2 real and 1 blank) were run at the WESP inlet, and two Pilat impactors (both real) were run at the WESP outlet. The target run time was 4 hrs for each run; however, several runs were curtailed due to various operational problems. All impactor runs were at least 2 hrs in duration. After the first week of pilot combustor testing, certain stages of the Pilat impactors were replaced to achieve smaller cutpoints. For all of the tests, the 0 stage of the Brink impactor was removed and used as a lab weighing control. Stage 6 was added to the Brink impactor to achieve the smallest possible cutpoints.

During all of the pilot combustor tests, the impactors were heated to 220-240°F. This temperature range is sufficient to prevent water condensation within the impactor, but still low enough to avoid any appreciable loss of collected acid by vaporization.

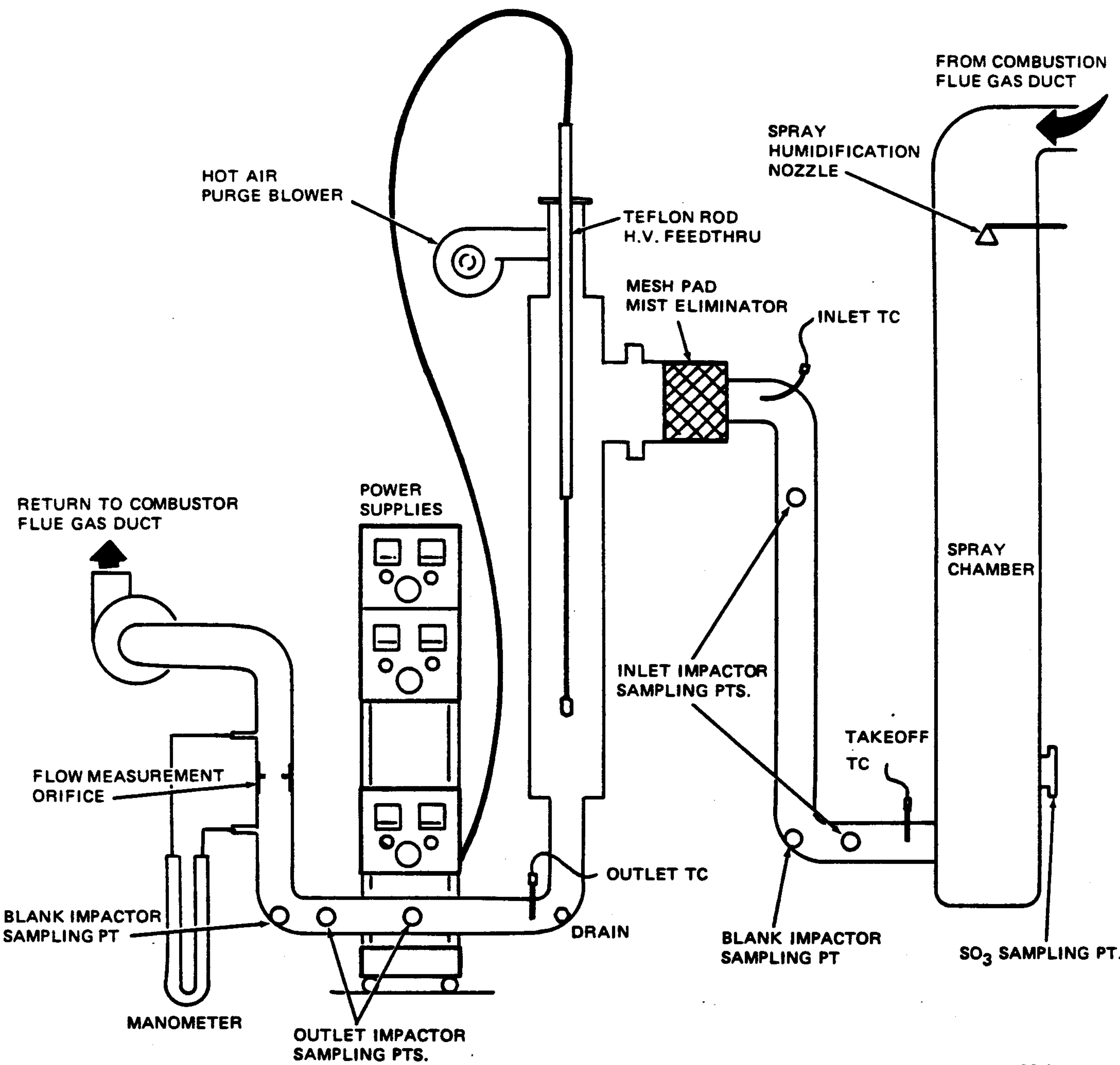

Figure 5. Sketch of Modified WESP System Used in Pilot Combustor Tests.

Prior to each run, a voltage-current curve was obtained in order to verify proper electrical operation of the WESP. Typical voltage-current curves are shown in Figures 6-9. Based on initial V-I curves, it was decided to operate at an applied voltage of 60 kV, which produced an operating current of 1.5 mA with flue gas flow at a temperature of 140-150°F. However, just after this operating point was established, the 60 kV power supply failed and was replaced with a 50 kV power supply. In order to achieve the same operating current (nominally 1.5 mA), it was therefore necessary to operate the 50 kV supply at a setting that was off scale on the voltage meter. To determine the actual applied voltage, the power supply was calibrated later. Although previous voltage-current curves suggested a value of 60 ± 5 kV for the applied voltage, the subsequent calibration revealed that the true value was 68 kV. The operating current varied between 1.0 and 1.85 mA depending upon the inlet mist loading and the cleanliness of the discharge electrode. A value of 1.5 mA corresponds to a current density of about 200 $\mu A/ft^2$. This is approximately a factor of 4-7 times greater than typical operating current densities for modern dry ESPs.

At the average gas flow of 167 acfm (flue gas plus purge), the WESP had a specific collecting area (SCA) of 44 ft^2/KACFM. This is approximately a factor of 4-8 times smaller than the SCA of modern dry ESPs used in typical fly ash applications.

Tables 1 and 2 give summaries of the inlet and outlet impactor runs performed during the weeks of August 14 and August 28. The tables include cumulative mass loadings for particles < 1 μm, < 5 μm, and total. The averages and standard deviations on these values are also included to give an indication of the variability in the runs. These averages may not agree precisely with the values determined by the computerized data reduction due to the outlier analysis used in the computer program. The variations in the inlet loadings are presumably due to fluctuations in the amount of condensed mist reaching the WESP system.

The acid condensation process is extremely sensitive to changes in system temperatures and the performance of the spray humidification system. Since the total inlet loading was significantly higher during the week of August 28 (16.3 mg/acm versus 8.59 mg/acm for the week of August 14), these data sets were treated separately in the computerized data analysis.

Figure 10 shows the inlet and outlet cumulative mass loading curves produced by the computer analysis of the data obtained under the conditions discussed above. The curves for the week of August 14 represent the averages for the 6 real inlet Brink runs and the 4 outlet Pilat runs detailed in Table 1. The curves for the week of August 28 represent the averages for the 8 real inlet Brink runs and the 8 outlet Pilat runs detailed in Table 2. All of the blank impactor runs showed very low weight gains indicating that the heating to 230°F was sufficient to prevent condensation or adsorption of acid or water vapor. (It should be noted, however, that all of the acid should have already been condensed in the spray chamber.) As the 90% confidence intervals on the data indicate, the impactor data were reasonably consistent.

The fractional collection efficiency curve computed from the inlet and outlet impactor data is shown in Figure 11. The curve appears reasonable for particle sizes up to about 2 μm. Above 2 μm, however, there appears to be an anomalous increase in penetration (decrease in collection efficiency) for the week of August 14. This anomaly is also evident in the data for the week of August 28. This may be partly attributed to the fact that there is very little particulate mass in this

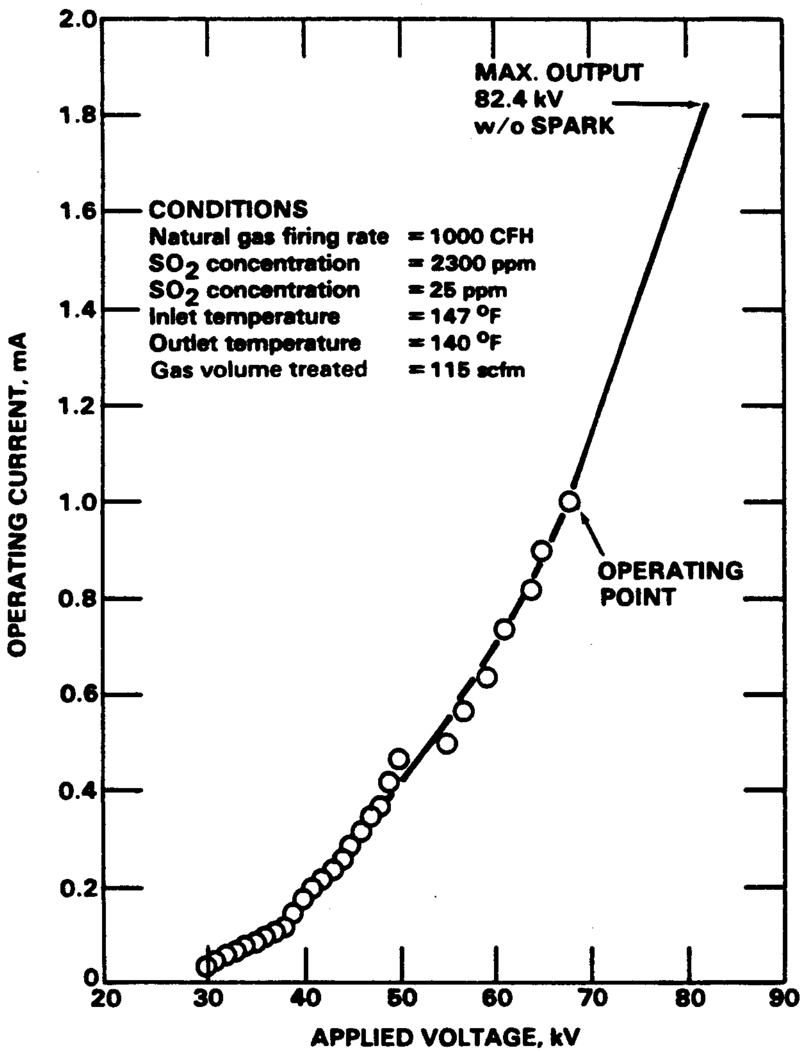

Figure 6. Voltage-Current Curve with Gas Firing - 8/16/89.

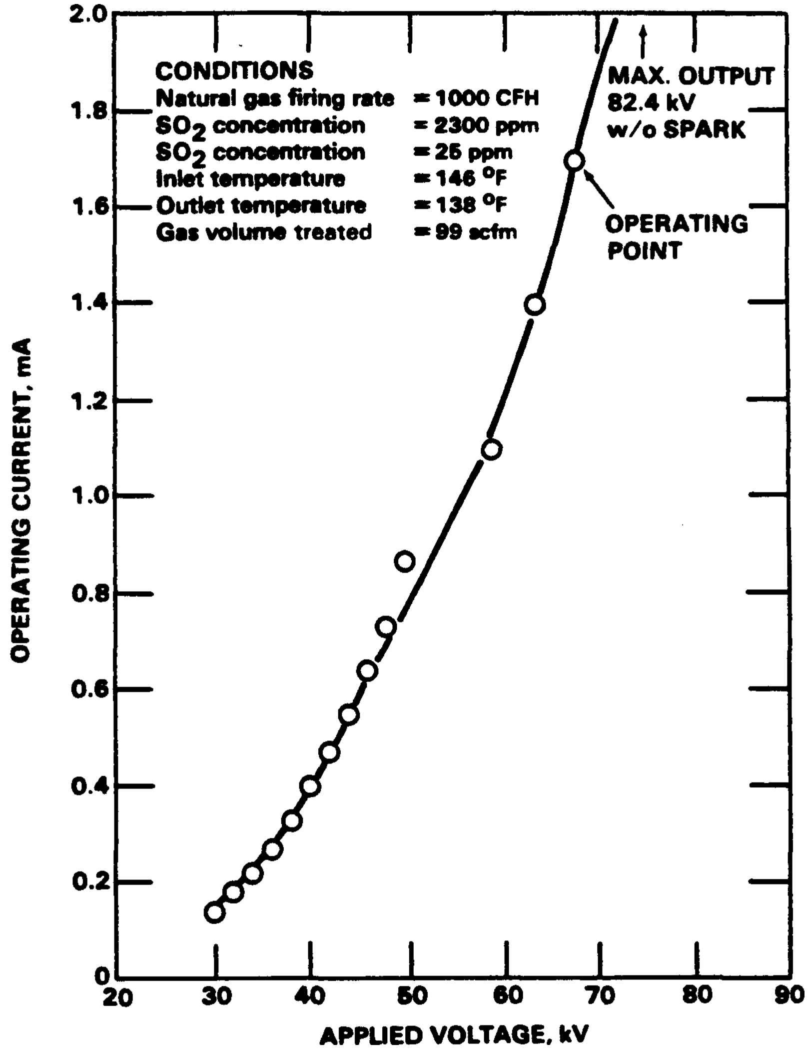

Figure 7. Voltage-Current Curve with Gas Firing - 8/18/89.

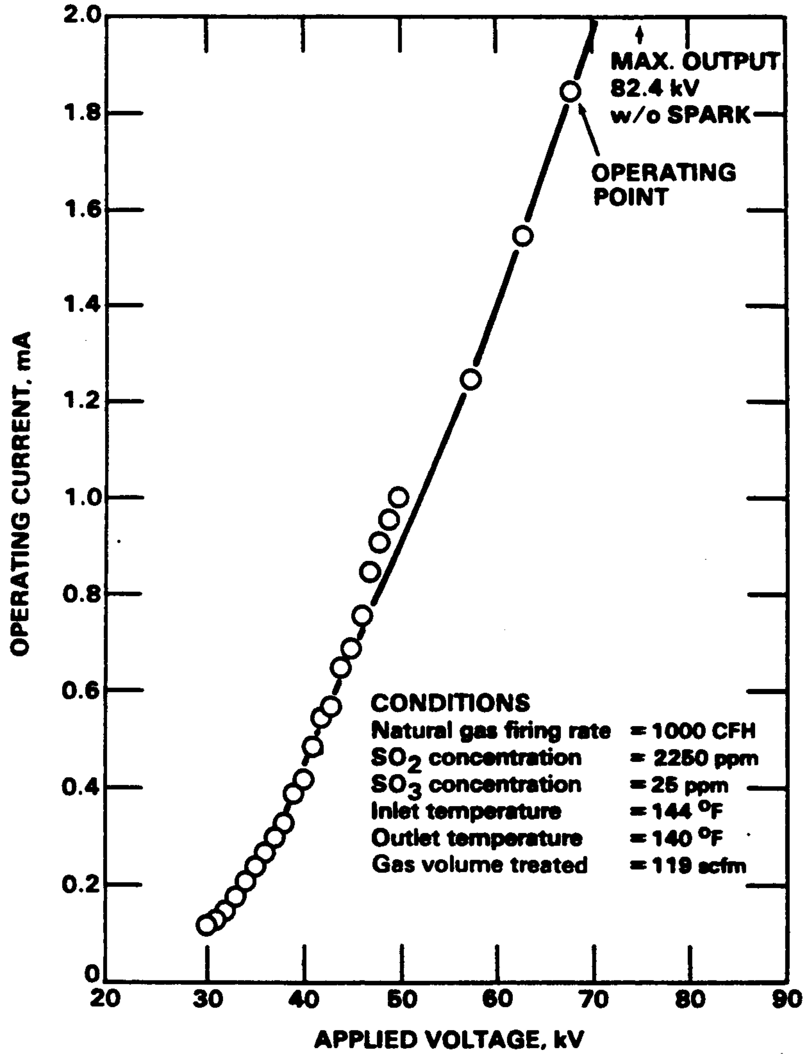

Figure 8. Voltage-Current Curve with Gas Firing - 8/31/89.

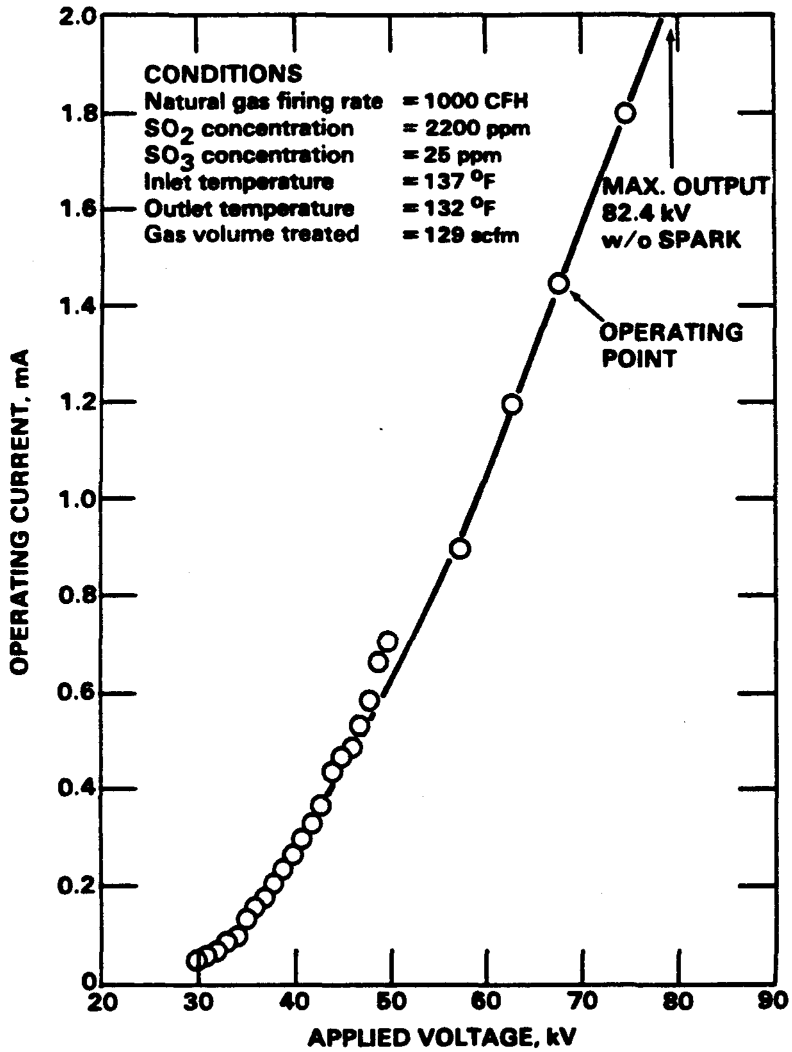

Figure 9. Voltage-Current Curve with Gas Firing - 9/1/89.

Table 1. Summary of Impactor Data for Week of August 14 (SO_2-Doped Natural Gas)

Inlet Impactor Runs

Run No. F318 -	Date	Start Time	End Time	Temp., °F	Gas Flow acfm	Mass Loading, mg/acm Uncorrected (Corrected)[a] <1 μm		<5 μm		Total		MMD, μm
95-1	8/16	13:00	14:00	169	78	11.3	(5.79)	23.7	(11.8)	24.1	(12.1)	1.1
95-3	8/16	13:02	14:02	169	78	3.07	(1.56)	17.5	(8.59)	19.9	(9.76)	2.4
103	8/17	10:36	14:36	169	78	3.56	(1.82)	9.66	(4.85)	13.4	(6.74)	2.7
105	8/17	10:43	14:43	169	78	4.78	(2.39)	14.0	(6.86)	14.8	(7.24)	1.8
110	8/18	9:25	13:25	169	78	3.77	(1.90)	10.3	(5.12)	11.3	(5.60)	1.9
112	8/18	9:28	13:28	169	78	7.23	(3.75)	20.0	(9.76)	20.8	(10.1)	1.4
Average				169	78	5.62	(2.87)	15.9	(7.83)	17.4	(8.59)	1.9
Standard Deviation				0	0	3.15	(1.63)	5.55	(2.73)	4.95	(2.46)	0.60
Relative Standard Deviation, %				0	0	56.0	(56.8)	34.9	(34.8)	28.5	(28.6)	31.5

Outlet Impactor Runs

Run No. F318 -	Date	Start Time	End Time	Temp., °F	Gas Flow acfm	Mass Loading, mg/acm <1 μm	<5 μm	Total	MMD, μm
95-4	8/16	13:03	14:03	121	167	-[b]	-[b]	-[b]	-[b]
95-5	8/16	13:04	14:04	121	167	-[b]	-[b]	-[b]	-[b]
106	8/17	10:38	14:38	120	143	0.45	1.00	1.79	3.7
107	8/17	10:44	14:44	120	143	0.08	0.35	1.26	10.3
113	8/18	9:27	13:27	127	143	0.12	0.65	1.47	6.7
114	8/18	9:30	13:30	127	143	0.40	0.85	1.48	2.9
Average				123	151	0.26	0.71	1.50	5.9
Standard Deviation				3.4	12.4	0.19	0.28	0.22	3.4
Relative Standard Deviation, %				2.8	8.2	72.9	39.6	14.6	56.9
Calculated Cumulative Collection Efficiency, %						90.9	90.9	82.5	
Cumulative Collection Efficiency for 8/16, %						92.9[c]	93.0[c]	86.3[c]	
Cumulative Collection Efficiency for 8/17, %						87.4	88.5	78.2	
Cumulative Collection Efficiency for 8/18, %						90.8	89.9	81.2	

[a]Values in parentheses are corrected for dilution, and adjusted to final (diluted) gas composition and temperature.
[b]Data not obtained due to weighing error.
[c]Calculated using average outlet loading.

Table 2. Summary of Impactor Data for Week of August 28 (SO_2-Doped Natural Gas)

Inlet Impactor Runs

Run No. F318 -	Date	Start Time	End Time	Temp., °F	Gas Flow acfm	Mass Loading, mg/acm Uncorrected (Corrected)[a] <1 μm	<5 μm	Total	MMD, μm
121	8/29	14:00	16:00	173	106	15.2 (7.74)	24.0 (12.1)	25.6 (12.9)	0.79
123	8/29	14:05	16:05	173	106	9.21 (4.52)	13.3 (6.54)	14.2 (6.97)	0.70
129	8/30	11:32	14:32	172	105	47.7 (23.9)	59.7 (29.6)	59.9 (29.7)	0.78
131	8/30	11:37	14:37	172	105	2.56 (1.27)	16.8 (8.13)	20.4 (9.88)	2.7
138	8/31	10:00	-[b]	173	89	-[b]	-[b]	-[b]	-[b]
140	8/31	10:10	13:10	173	89	34.8 (17.0)	62.1 (29.7)	63.8 (30.5)	0.94
147	9/1	10:08	14:08	171	80	2.30 (1.17)	14.4 (7.22)	19.7 (9.76)	3.7
149	9/1	10:12	14:12	171	80	11.3 (5.42)	28.6 (13.7)	29.7 (14.2)	1.2
Average				172	95	17.6 (8.72)	31.3 (15.3)	33.3 (16.3)	1.5
Standard Deviation				0.9	11.7	17.2 (8.57)	20.9 (10.1)	20.1 (9.73)	1.18
Relative Standard Deviation, %				0.5	12.4	97.8 (98.3)	67.0 (66.3)	60.4 (59.7)	78.6

Outlet Impactor Runs

Run No. F318 -	Date	Start Time	End Time	Temp., °F	Gas Flow acfm	Mass Loading, mg/acm ≤1 μm	≤5 μm	Total	MMD, μm
124	8/29	14:10	16:10	137	190	2.02	2.34	2.60	0.41
125	8/29	14:00	16:00	137	190	2.63	3.00	3.06	0.42
132	8/30	11:38	14:38	139	173	2.85	3.40	3.60	0.46
133	8/30	11:40	14:40	139	173	1.42	1.78	1.88	0.52
141	8/31	10:10	12:10	147	179	2.61	2.91	3.03	0.35
142	8/31	10:00	12:00	147	179	1.70	1.94	1.98	0.46
150	9/1	10:14	14:14	123	189	1.06	1.33	1.60	0.60
151	9/1	10:14	14:14	123	189	2.05	2.37	2.45	0.38
Average				137	183	2.04	2.38	2.52	0.45
Standard Deviation				9.2	7.6	0.63	0.69	0.68	0.08
Relative Standard Deviation, %				6.7	4.1	30.9	29.1	27.1	17.8
Calculated Cumulative Collection Efficiency, %						76.6	84.4	84.5	
Cumulative Collection Efficiency for 8/29, %						62.1	71.4	71.5	
Cumulative Collection Efficiency for 8/30, %						83.0	86.3	86.2	
Cumulative Collection Efficiency for 8/31, %						87.3	91.8	91.8	
Cumulative Collection Efficiency for 9/1, %						52.8	82.3	83.1	

[a]Values in parentheses are corrected for dilution, and adjusted to final (diluted) gas composition and temperature.
[b]Blown run - jets clogged.

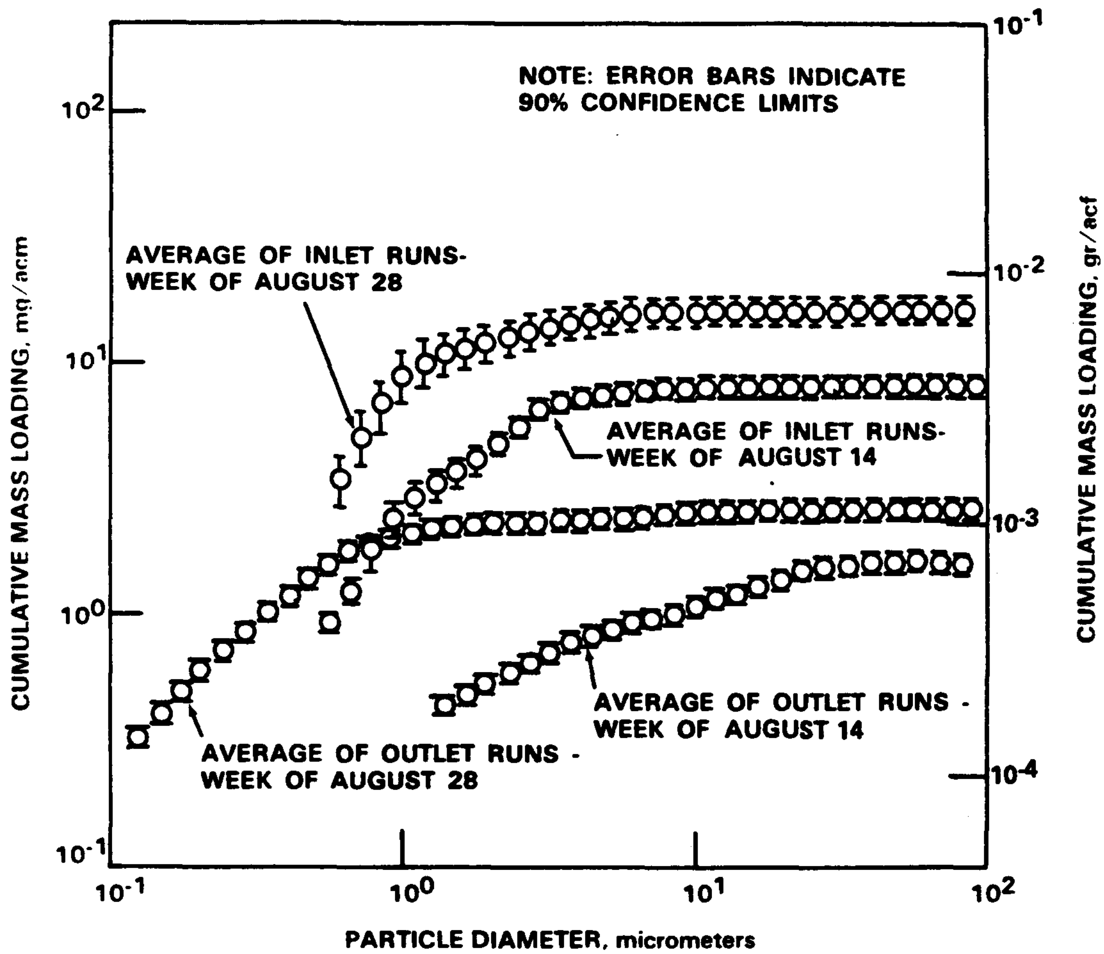

Figure 10. Cumulative Mass Loading Curves Obtained at WESP Inlet and Outlet with Acid Mist Generated from SO_2-Doped Natural Gas.

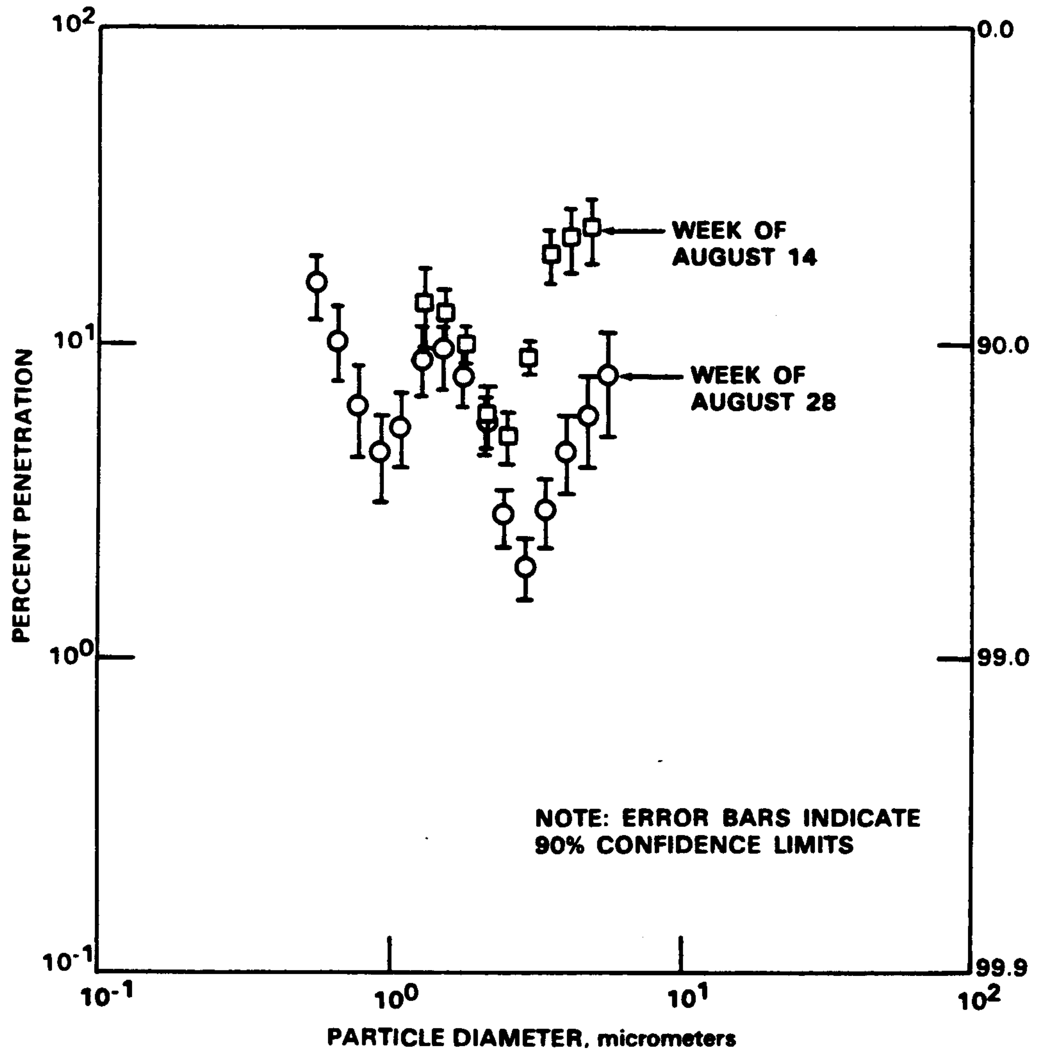

Figure 11. Fractional Collection Efficiency Curves Determined from Inlet and Outlet Impactor Runs with Acid Mist Generated from SO_2-Doped Natural Gas.

size range at the inlet (see Figure 10). Also, the fact that the sampling was not isokinetic would tend to bias the data in this size range. However, the data below 2 μm would not be affected. In any event, it is clear that the WESP achieved excellent collection efficiencies for particles below 2 μm, which would make up most of the acid mist. For the particle sizes resolved in this range (< 2 μm), the fractional efficiency varies from 85% to 95%.

4.2. Tests with Acid Mist Plus Fly Ash

During these tests the WESP system was evaluated with a combination of acid mist and fly ash generated by co-firing coal and SO_2-doped natural gas in the pilot combustor. The setup of the WESP system was essentially the same as that used during the tests with acid mist only. Coal was fired at a rate of 2 lb/hr, and natural gas was fired at a rate of 970 CFH, so that the total heat input was maintained at the same level used previously. Since the combination of fly ash and acid mist produced a higher mass loading than the mist alone, the impactor run times were reduced to 1 hr. The impactor setup was also changed from 3 Brink (2 real and 1 blank) and 2 University of Washington (both real) impactors to 2 Brink (both real) and 3 University of Washington (2 real and 1 blank) impactors. This adjustment was made because it was realized that there was a greater potential for gas-phase interferences with the University of Washington impactors due to their larger substrate surface areas and the higher ratio of gas-to-solids at the outlet. This change made no difference in the results, as the blank corrections were still negligible.

During this series of tests, it was immediately noted that the WESP could not be operated under the same electrical conditions achieved in the mist-only tests. Voltage-current curves, such as those shown in Figures 12 and 13, showed that the voltage could be increased to 60 kV, but it was not possible to maintain long-term, stable operation at this voltage. A voltage of 45 kV was selected as the operating point, but it may have been possible to operate at a somewhat higher voltage without sparkover. Also, vibration of the discharge electrode probably caused some sparking that would not have occurred otherwise. At the applied voltage of 45 kV, the operating current varied from 0.44 to 0.50 mA, corresponding to a current density of 60-68 $\mu A/ft^2$. This is still somewhat higher than that typically achieved in a dry fly ash ESP.

Table 3 gives a summary of the impactor runs performed while collecting acid mist and fly ash during the week of September 11. Again, there was considerable variability in the submicron mass loadings, although the total mass loadings had comparatively small relative standard deviations (23.3% on the inlet and 32.2% on the outlet). This could be attributable to the sensitivity of the acid mist condensation to the process conditions. The fly ash loadings would not be so sensitive and would tend to make the total loading more stable. Comparing the results to the mist-only case, the cumulative collection efficiencies are significantly lower, as shown below:

	Cumulative collection efficiencies, %		
	≤ 1 μm	≤ 5 μm	Total
Mist only (wk of 8/14)	90.9	90.9	82.5
Mist only (wk of 8/28)	76.6	84.4	84.5
Mist + fly ash (wk of 9/11)	42.7	77.1	77.6

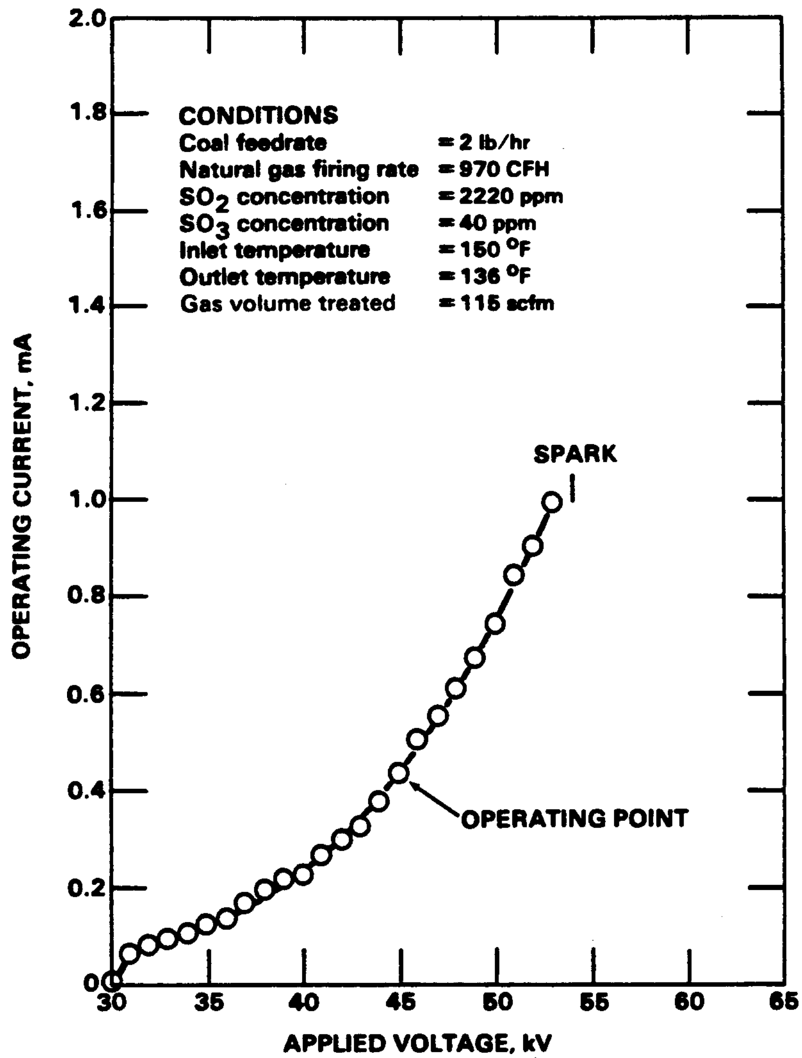

Figure 12. Voltage-Current Curve with Coal Firing - 9/12/89.

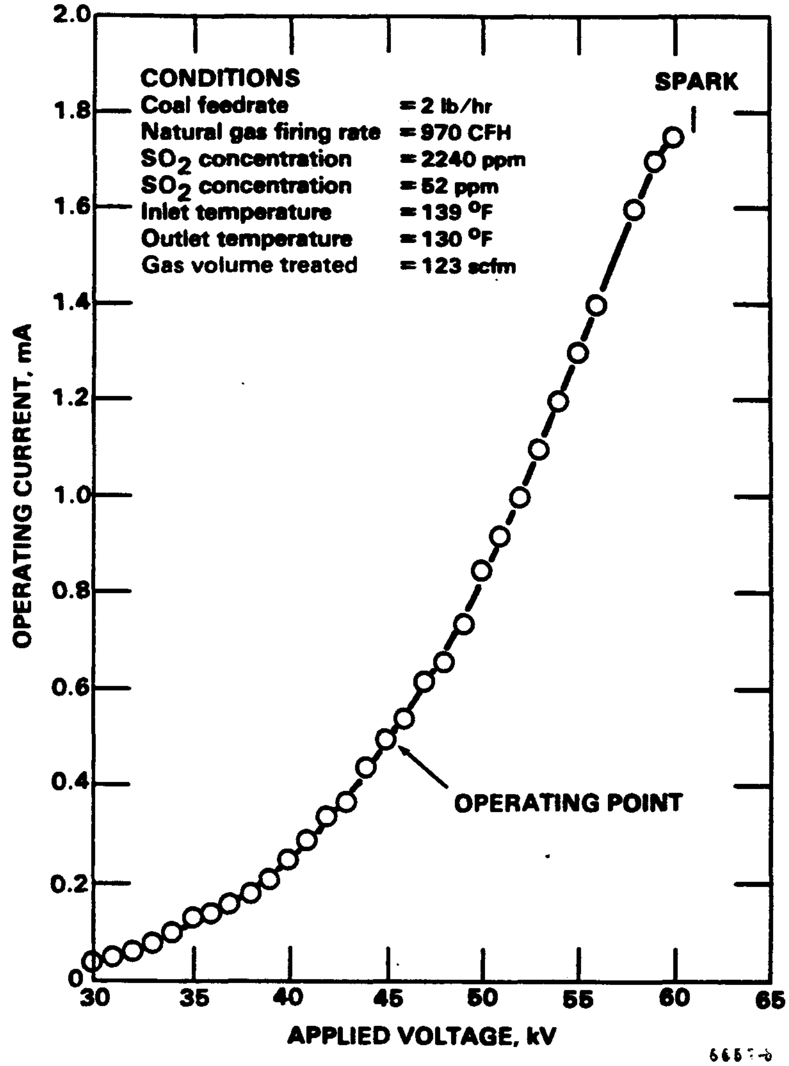

Figure 13. Voltage-Current Curve with Coal Firing - 9/15/89.

Table 3. Summary of Impactor Data for Week of September 11 (Coal Firing)

Inlet Impactor Runs

Run No. F318 -	Date	Start Time	End Time	Temp., °F	Gas Flow acfm	Mass Loading, mg/acm Uncorrected (Corrected)[a] <1 μm	<5 μm	Total	MMD, μm
157-1	9/12	13:50	14:50	170	78	9.36 (4.82)	34.3 (17.6)	37.8 (19.4)	1.8
157-2	9/12	13:53	14:53	170	78	31.7 (16.3)	68.3 (34.9)	73.5 (37.5)	1.1
159-1	9/13	10:08	11:08	172	78	8.57 (4.41)	40.3 (20.6)	49.7 (25.3)	2.5
159-2	9/13	10:10	11:10	172	78	6.59 (3.42)	51.9 (26.5)	62.4 (31.8)	2.8
160-1	9/14	10:15	11:15	175	107	8.04 (4.14)	26.3 (13.4)	35.6 (18.1)	2.7
160-2	9/14	10:17	11:17	175	107	12.7 (6.61)	49.8 (25.4)	57.9 (29.5)	2.0
161-1	9/15	10:07	11:07	164	105	14.5 (7.37)	47.3 (23.9)	58.9 (29.7)	2.6
161-2	9/15	10:08	11:08	164	105	8.27 (4.31)	50.9 (25.5)	58.3 (29.2)	2.3
Average				170	92	12.5 (6.42)	46.1 (23.5)	54.3 (27.6)	2.2
Standard Deviation				4.3	15.0	8.2 (4.20)	12.7 (6.46)	12.7 (6.42)	0.57
Relative Standard Deviation, %				2.5	16.3	65.6 (65.5)	27.6 (27.5)	23.4 (23.3)	25.9

Outlet Impactor Runs

Run No. F318 -	Date	Start Time	End Time	Temp., °F	Gas Flow acfm	Mass Loading, mg/acm <1 μm	<5 μm	Total	MMD, μm
157-3	9/12	13:50	14:50	130	167	3.83	4.91	5.60	0.48
157-4	9/12	13:53	14:53	130	167	2.12	3.51	4.04	0.91
159-3	9/13	10:10	11:10	132	168	6.19	7.34	7.90	0.43
159-4	9/13	10:10	11:10	132	168	6.69	8.27	9.39	0.49
160-3	9/14	10:15	11:15	132	180	1.67	4.32	5.45	1.9
160-4	9/14	10:17	11:17	132	180	1.69	3.25	4.38	1.6
161-3	9/15	10:07	11:07	135	181	5.82	7.47	8.03	0.37
161-4	9/15	10:09	11:09	135	181	1.46	3.95	4.66	1.8
Average				132	174	3.68	5.38	6.18	1.0
Standard Deviation				1.9	7.0	2.25	2.00	1.99	0.66
Relative Standard Deviation, %				1.4	4.0	61.0	37.2	32.2	66.2
Calculated Cumulative Collection Efficiency, %						42.7	77.1	77.6	
Cumulative Collection Efficiency for 9/12, %						71.8	84.0	83.1	
Cumulative Collection Efficiency for 9/13, %						6.0[b]	66.9	69.7	
Cumulative Collection Efficiency for 9/14, %						68.7	80.5	79.3	
Cumulative Collection Efficiency for 9/15 %						37.7	76.9	78.5	

[a]Values in parentheses are corrected for dilution, and adjusted to final (diluted) gas composition and temperature.
[b]Computed using average outlet loading.

Figure 14 shows the inlet and outlet cumulative mass loading curves produced by the computer analysis of the mist + fly ash data for the week of September 11. These curves represent the averages for the 8 real inlet Brink runs and the 8 real outlet Pilat runs detailed in Table 3. Again, all of the blank impactor runs showed very low weight gains indicating there was no problem with vapor-phase interferences. Again, the 90% confidence intervals indicate good consistency in the data.

The fractional collection efficiency curve computed from the inlet and outlet impactor data is shown in Figure 15. Again, there is an apparent anomaly in the results for particle sizes above 1-2 μm. This may be attributable to the small mass in this size range and non-isokinetic sampling, which would not affect the results for smaller particle sizes. In any case, it is clear that the WESP system achieved good collection efficiency for particles in the submicron size range (from 61% at 0.67 μm to 86% at 2 μm). This would effectively eliminate much of the source of opacity problems (e.g., the blue plume phenomenon).

5. MATHEMATICAL MODELING OF WESP PROCESS

To assist in the interpretation of test results and optimization of the WESP process, a computer model was developed. Initially, two different cylindrical geometry models were considered. The first model was basically the same as the standard SRI/EPA ESP model (6), except that it was converted to cylindrical geometry. This is a Deutschian model with an empirical correction to the calculated migration velocities based on fractional efficiency data for ESPs collecting fly ash. The standard version of this model also includes empirical corrections for non-uniform gas flow, sneakage, and rapping reentrainment, but none of these corrections were used in this study since they are not applicable to the WESP process.

The second model was a so-called "current-seeking" model which derives the current in each length increment based on the applied voltage and the calculated space charge in the interelectrode space. In this model, the current is predicted using the Townsend Equation (7). This equation applies only in the region near corona start, which is far removed from the operating conditions of the WESP during this test program. Therefore, the current-seeking model may be expected to be less accurate than the standard "current-specific" model. This expectation was confirmed by initial comparisons with the laboratory data, so further model development and comparisons were focused on the standard, current-specific model.

5.1. Comparison of Mathematical Model to Test Data

The current-specific model was used to predict the WESP collection efficiency for all three sets of pilot combustor tests: two sets with mist only (weeks of 8/14 and 8/28), and one set with mist plus fly ash (week of 9/11). The average operating conditions used for the model runs are given in Table 4. Since the primary objective was to determine the model's ability to predict collection of particles in the size range of the acid mist, comparisons were made on a cumulative basis for all particles below 1 μm, below 5 μm, and total. These comparisons are summarized in Tables 5, 6, and 7.

For the first comparison shown in Table 5, the model accurately predicts the overall collection efficiency (83.7% predicted versus 82.5% measured). However, the model underpredicts the cumulative efficiency at 5 μm (82.4% predicted versus 90.9% measured), and it vastly underpredicts the submicron efficiency (70.4% versus

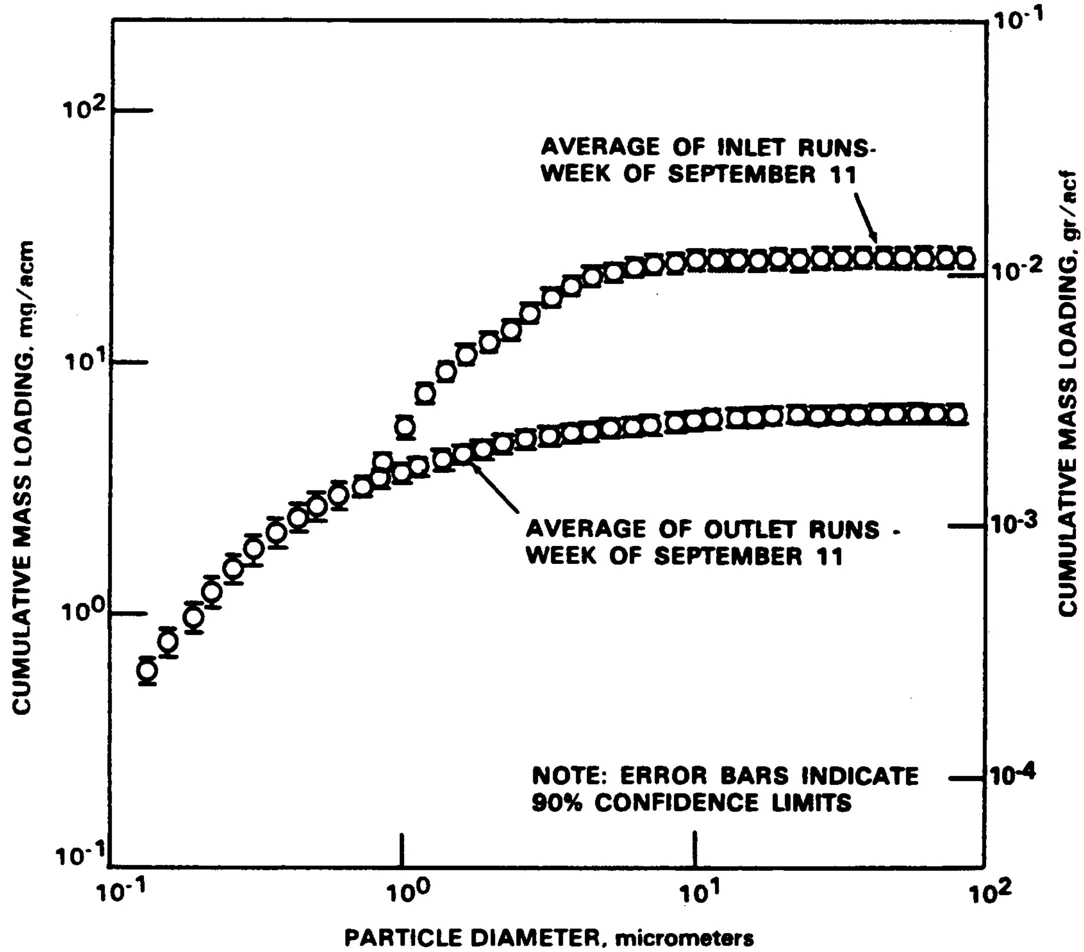

Figure 14. Cumulative Mass Loading Curves Obtained at WESP Inlet and Outlet with Fly Ash Plus Acid Mist Generated by Co-Firing Coal and SO_2-Doped Natural Gas.

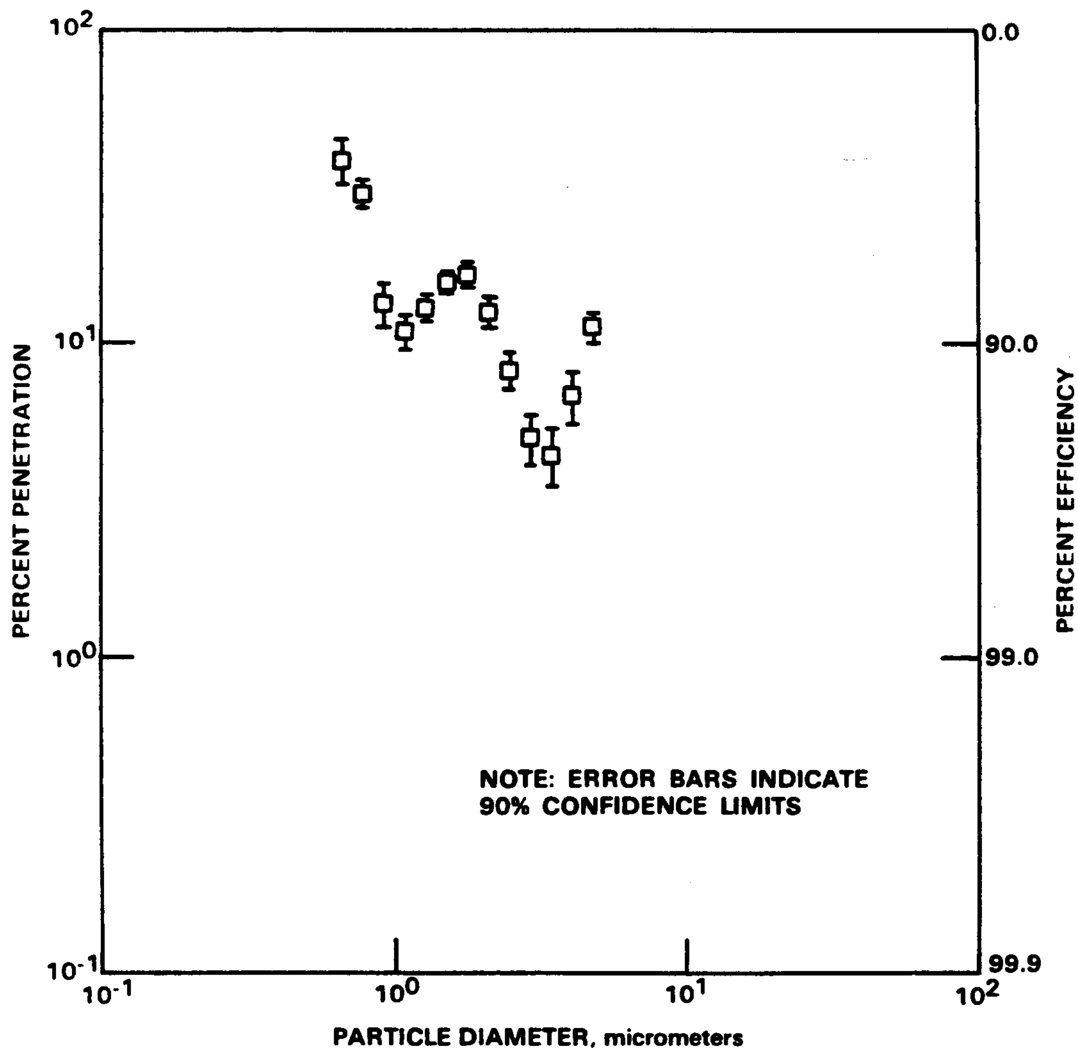

Figure 15. Fractional Collection Efficiency Curve Determined from Inlet and Outlet Impactor Runs with Fly Ash Plus Acid Mist Generated by Co-Firing Coal and SO_2-Doped Natural Gas.

Table 4. Summary of Average Operating Data Used in Model Runs

WESP Geometry - Wire-Pipe
Pipe ID = 8.15 in.
Wire diameter = 0.125 in.
Energized length - 3.46 ft

Average Conditions for Week of	August 14	August 28	September 11
Particulate collected	Mist only	Mist only	Mist + fly ash
Flue gas flowrate, acfm	151	183	174
SCA, ft^2/kacfm	48.9	40.3	42.4
Gas velocity, ft/sec	6.9	8.4	8.0
Residence time, sec	0.50	0.41	0.43
Flue gas percent oxygen	11.3	12.5	12.3
Flue gas percent carbon dioxide	4.1	3.5	3.6
Flue gas percent nitrogen	73.7	73.3	73.3
Flue gas percent water	10.9	10.7	10.8
Inlet temperature, °F	130	130	130
Inlet mass loading, mg/acm	8.59	16.3	27.6
Inlet mass loading, gr/acf	0.00375	0.00711	0.0120
Inlet mmd, microns	1.9	1.5	2.2
Applied voltage, kV	68	68	45
Operating current, mA	1.7	1.85	0.50

Table 5. Comparison of Current-Specific Model Predictions with Mist-Only Data for Week of August 14

		Measured	Predicted	% Difference
Inlet Cumulative Mass, mg/acm				
	< 1 μm	2.87	-	-
	< 5 μm	7.83	-	-
	Total	8.59	-	-
Outlet Cumulative Mass, mg/acm				
	< 1 μm	0.26	0.85	106
	< 5 μm	0.71	1.38	64.1
	Total	1.50	1.40	6.9
Cumulative Collection Efficiency, %				
	< 1 μm	90.9	70.4	25.4
	< 5 μm	90.9	82.4	9.8
	Total	82.5	83.7	1.4

90.9%). The most likely explanation for the disagreement in the fine particle efficiency appears to be a problem with the impactor data in this size range. The primary justification for this explanation is that the measured efficiency does not decrease with decreasing particle size as expected. Decreasing collection efficiencies were evident in the latter two data sets, further suggesting a problem with the first set. Nevertheless, the first data set appears to give a reasonable overall efficiency that agrees reasonably well with the model prediction.

For the second comparison shown in Table 6, the model slightly underpredicts the cumulative collection efficiencies, but the comparison is reasonably good, as indicated in the following summary:

< 1 μm - 76.6% measured versus 71.1% predicted (7.4% difference)

< 5 μm - 84.4% measured versus 79.4% predicted (6.1% difference)

Total - 84.5% measured versus 80.6% predicted (4.7% difference)

The inlet size distribution for this data set contained a larger mass of fine particles (mmd of 1.5 μm versus 1.9 μm for the first data set). According to the model, this was more than enough to offset the slightly higher operating current in this case (1.85 versus 1.70 mA), resulting in a predicted overall efficiency of 80.6%, compared to 83.7% for the first data set. The measured efficiencies showed the opposite trend (84.5% for the second data set, compared to 82.5% for the first). Nevertheless, the overall agreement between predicted and measured efficiencies is not bad for both of the first two data sets, with percent differences of only 1.4% and 4.7%.

Table 7 gives a summary comparison for the final, mist plus fly ash, data set. For this data set, the submicron fraction shows better agreement, as shown in the following:

< 1 μm - 42.7% measured versus 38.0% predicted (11.6% difference)

< 5 μm - 77.1% measured versus 55.7% predicted (32.2% difference)

Total - 77.6% measured versus 59.8% predicted (25.9% difference)

For this case, it was estimated that approximately 60% of the inlet mass was acid mist, and about 40% was fly ash. The presence of the fly ash resulted in a larger mmd for the inlet aerosol in this case (2.2 μm versus 1.5-1.9 μm for the mist-only cases). There was a loading of about 4.1 mg/acm (or about 15% of the total mass) of particles larger than 5 μm. This causes some concern because it is approaching the size range where the mist eliminator could have an effect. Previous data obtained with the DES aerosol showed that the mist eliminator did not collect any particles smaller than 5 μm; however, the mist eliminator was about 38% efficient for droplets in the 5 μm to 10 μm range. Thus, the mist eliminator could have effectively reduced the inlet loading to the WESP by 4.1 x 0.38 = 1.6 mg/acm. This would result in the measured efficiency being reduced from 77.6% to 76.2%.

Table 6. Comparison of Current-Specific Model Predictions with Mist-Only Data for Week of August 28

		Measured	Predicted	% Difference
Inlet Cumulative Mass, mg/acm				
	< 1 μm	8.72	-	-
	< 5 μm	15.3	-	-
	Total	16.3	-	-
Outlet Cumulative Mass, mg/acm				
	< 1 μm	2.04	2.52	21.0
	< 5 μm	2.38	3.15	27.8
	Total	2.52	3.16	22.5
Cumulative Collection Efficiency, %				
	< 1 μm	76.6	71.1	7.4
	< 5 μm	84.4	79.4	6.1
	Total	84.5	80.6	4.7

Table 7. Comparison of Current-Specific Model Predictions with Mist Plus Fly Ash Data for Week of September 11

		Measured	Predicted	% Difference
Inlet Cumulative Mass, mg/acm				
	< 1 μm	6.42	-	-
	< 5 μm	23.5(14.7)*	-	-
	Total	27.6(17.7)*	-	-
Outlet Cumulative Mass, mg/acm				
	< 1 μm	3.68	3.98	7.8
	< 5 μm	5.38	10.4	63.6
	Total	6.18	11.1	56.9
Cumulative Collection Efficiency, %				
	< 1 μm	42.7	38.0	11.6
	< 5 μm	77.1(63.4)*	55.7	32.2(12.9)*
	Total	77.6(65.1)*	59.8	25.9(8.5)*

*Corrected for particulate mass collected by mist eliminator (see text for discussion).

The mist eliminator efficiency cited above was measured in the laboratory with an air velocity of only 3 ft/sec. In the pilot combustor tests, the WESP was operated at a gas velocity of 6.9-8.4 ft/sec. This would tend to increase the mist eliminator collection efficiency and extend the particle size range affected to smaller sizes. According to the manufacturer's literature, the affected size range would be extended to 2 μm at a gas velocity of 20 ft/sec. These figures suggest that the lower limit of the affected size range is inversely proportional to the square root of gas velocity (as expected from impaction theory) with a proportionality constant given by

$$K = D(V)^{0.5} = 5(3)^{0.5} = 2(20)^{0.5} \simeq 8.8$$

The limiting particle size at 8 ft/sec is then given by $D = 8.8/(8)^{0.5} = 3.1$ μm.

At the WESP inlet sampling location, the mass loading of particles larger than 3.1 μm is about 17.7 mg/acm. The fraction of these particles that was collected by the mist eliminator may be calculated from the following relation (8):

$$\eta = 1 - \exp\left[-K d_p^2 U_g\right]$$

where d_p is the particle diameter and U_g is the superficial gas velocity. From the previous laboratory data:

$$U_g = 3 \text{ ft/sec},\ d_p = (5 \times 10)^{0.5} = 7\ \mu m,\ \eta = 0.38, \text{ and } K = 0.00325.$$

For the mist-plus-fly ash data, $U_g = 8$ ft/sec, $d_p = (3.1 \times 10)^{0.5} = 5.6$ μm, and $\eta = 0.56$ (56% efficiency).

This would reduce the inlet mass loading by 0.56 x 17.7 mg/acm = 9.9 mg/acm, resulting in a corrected WESP collection efficiency of 65.1%, compared to an uncorrected value of 77.6%. Similarly the cumulative efficiency for particles smaller than 5 μm is adjusted from 77.1% to 63.4%. The submicron efficiency is not affected since the mist eliminator cannot collect such fine particles. Thus, the comparison of predicted and measured efficiencies becomes

< 1 μm - 42.7% measured versus 38.1% predicted

< 5 μm - 63.4% measured versus 55.7% predicted

Total - 65.1% measured versus 59.8% predicted

This is reasonably good agreement between the model and the data, considering the uncertainties involved.

5.2. Simulation of a Utility WESP Installation

Based on the impactor data and the computer modeling, it appears that an overall collection efficiency of 80% to 85% is achievable with an acid mist having an mmd of 1.5 to 1.9 μm. This is excellent performance considering that the WESP had an SCA of only 40 to 49 ft^2/kacfm and a treatment (residence) time of only 0.4 to 0.5 sec (at a gas velocity of 6.9 to 8.4 ft/sec). This performance is possible due to the excellent electrical operating conditions attainable in the mist-only condition (applied voltage of 68 kV and operating current density of 230 to 250 $\mu A/ft^2$).

With the addition of the fine fly ash particles, the WESP performance is diminished considerably (60% to 65% overall efficiency) due to the reduced operating voltage and current (45 kV and 67 $\mu A/ft^2$). Although these electrical operating conditions are still very good compared to those of dry ESPs, they are not sufficient to produce a high level of particulate collection in such a small device. Nevertheless, they may be adequate to alleviate opacity problems and the blue-plume phenomenon that is frequently associated with the acid mist. Also, the particulate collector and scrubber mist eliminator may reduce the fly ash loading to a level below that simulated here. The fly ash loading simulated here (about 11 mg/acm or 0.005 gr/acf) would correspond to a particulate collector efficiency of 95% in series with a scrubber/mist eliminator efficiency of 95%, based on the input ash in the coal. In an actual power plant, this efficiency would be significantly higher, and the ash loading to the WESP would be correspondingly lower. In an NSPS situation where the particulate collector efficiency is 99.7%, the ash loading to the WESP would be only 6% of that simulated here. Thus there would be much less reduction in the electrical operating conditions, and the WESP performance would be much closer to the mist-only condition (80% to 85% collection). Therefore, it appears likely that a utility WESP installation could operate at a control efficiency approaching 80% to 85% if there is a high efficiency particulate collector ahead of the scrubber.

It should be noted that a utility WESP could be operated at a gas velocity much higher than that used here. A WESP with an energized electrode length of only 10 ft could be operated at a gas velocity of 20 ft/sec and still provide the same treatment time used in this study. Since reentrainment is not a problem in a WESP, the higher gas velocity should not have any adverse impact on performance. With a WESP design based on 8-in. diameter tubes and a design gas velocity of 20 ft/sec, each tube could treat a gas flow of about 420 acfm. For a 500 MW plant producing 1,000,000 acfm of flue gas at 150°F, the required number of tubes would be 2380. With a tube length of 10 ft, this would provide an SCA of 50 ft^2/kacfm. Thus, this particular installation would be similar to the WESP test unit in its SCA and residence time, but it would operate at a gas velocity 2.5 times higher than that of the test unit. Model projections for the case of the commercial installation described above suggest a collection efficiency of 86.7% for mist only and 64.7% for 60% mist/40% fly ash. With a high-efficiency particulate collector ahead of the scrubber system, the actual performance should be closer to the 86.7% figure. The array of tubes used in the hypothetical WESP described above would fit within a cylindrical vessel having a diameter of about 36 ft. Thus, the hypothetical WESP could be retrofitted to an existing scrubber system. The total cross-sectional area of the WESP could be made smaller by using a more compact design (e.g., hexagonal tubes that share sides in an array).

6. CONCLUSIONS AND RECOMMENDATIONS

Under the conditions described previously, the WESP test unit achieved an overall collection efficiency, based on impactor measurements, of 82.5% to 84.5% while collecting acid mist only. These measurements were made in the absence of any fly ash in the system and with an acid mist having an mmd of 1.5 to 1.9 μm. Lower efficiencies would be expected in the presence of additional fine fly ash or with a finer size distribution of the mist. Nevertheless, these results show that a compact WESP is capable of substantial control of a fine acid mist, primarily due to the excellent electrical operating conditions that can be achieved.

The test results obtained with a combination of acid mist and fly ash are not definitive due to collection of fly ash by the mist eliminator ahead of the WESP. It may be argued that these ash particles would have been collected in the WESP anyway, in which case the measured efficiency of 77.6% may be a realistic estimate of expected performance. However, these data were obtained with electrical conditions that were apparently degraded significantly by the presence of the fly ash (45 kV compared to 68 kV for mist only, and 0.5 mA compared to 1.7 mA for mist only). This also complicates data interpretation because the fly ash loading was probably much higher than that expected after a high-efficiency particulate collector, scrubber, and mist eliminator. Thus, this degree of degradation probably would not be seen in an actual WESP installation.

The modeling performed to date has yielded substantial agreement with the test data in terms of overall collection efficiency. Failure to match the measured fractional efficiency curve appears to be attributable to the very low mass concentration in the large (> 2 μm) size range, which causes the data not to follow the expected trend with particle size. Despite this problem, the total mass loadings and overall measured efficiencies are believed to be reliable and are in substantial agreement with the modeling results. In the mist plus ash case, this is true only after correction of the inlet loading and efficiency for collection of ash in the mist eliminator.

A preliminary extrapolation of the modeling to a full-scale installation suggests that an overall collection efficiency as high as 86.7% may be achievable if the WESP is preceded by a high-efficiency particulate collector ahead of the scrubber. If the particulate collector is performing poorly and ash penetrates the scrubber/ mist eliminator system, this can significantly degrade performance as seen in the mist plus ash tests. Modeling of the worst-case scenario (40% ash by mass) shows that the overall collection efficiency can be degraded to 64.7%, primarily due to the degradation of the electrical operating conditions.

More accurate evaluations of expected WESP performance will require field data to determine the true size distribution and loading of the acid mist downstream from a scrubber/mist eliminator system. These measurements should be supplemented with additional computer modeling to assess the feasibility of the WESP for acid mist control in utility applications. The field measurements and additional modeling will be performed under Phase II of this contract if approval is received from DOE. Phase II would also include solicitation of utility participation in a follow-on demonstration of the WESP concept.

7. REFERENCES

1. D. Laslo, E. Bakke, and E. Chisholm. Limestone/Adipic Acid FGD and Stack Opacity Reduction Pilot Plant Tests at Big Rivers Electric Corporation. Peabody Process Systems Incorporated, Technical Report, 1984.

2. New Source Performance Standards: Electric Utility Steam Generating Units. Federal Register 44 (113):33580-33624 (June 11, 1979).

3. A. W. Wesa. Study of Various Sampling Procedures for Determining Particulate Emissions from Coal-Fired Steam Generators. Combustion, pp. 34-39, July 1977.

4. M. J. Krall, M. R. Fuchs, and W. D. Balfour. Characterization of Flue Gas Emissions from the PPSI FGD Pilot Plant, Technical Report - Vol. I. Radian Corporation, February 1983.

5. S. A. Jaasund. E-Tube Wet Electrostatic Precipitator - Leading Plywood Test Results. Geoenergy International Corporation, Report to Leading Plywood Corporation, 1988.

6. M. G. Faulkner and J. L. DuBard. A Mathematical Model of Electrostatic Precipitation, Revision 3. Volume I, Modeling and Programming, NTIS PB84-212-679. Volume II, User Manual, NTIS PB84-212-687. U.S. EPA, Research Triangle Park, NC, Grant No. R806216, May 1982.

7. H. J. White. Industrial Electrostatic Precipitation. Addison-Wesley, Reading, MA, pp. 94-95, 1963

8. R. M. Bethea. Air Pollution Control Technology. Van Nostrand Reinhold, New York, NY, pp. 325-326, 1978.